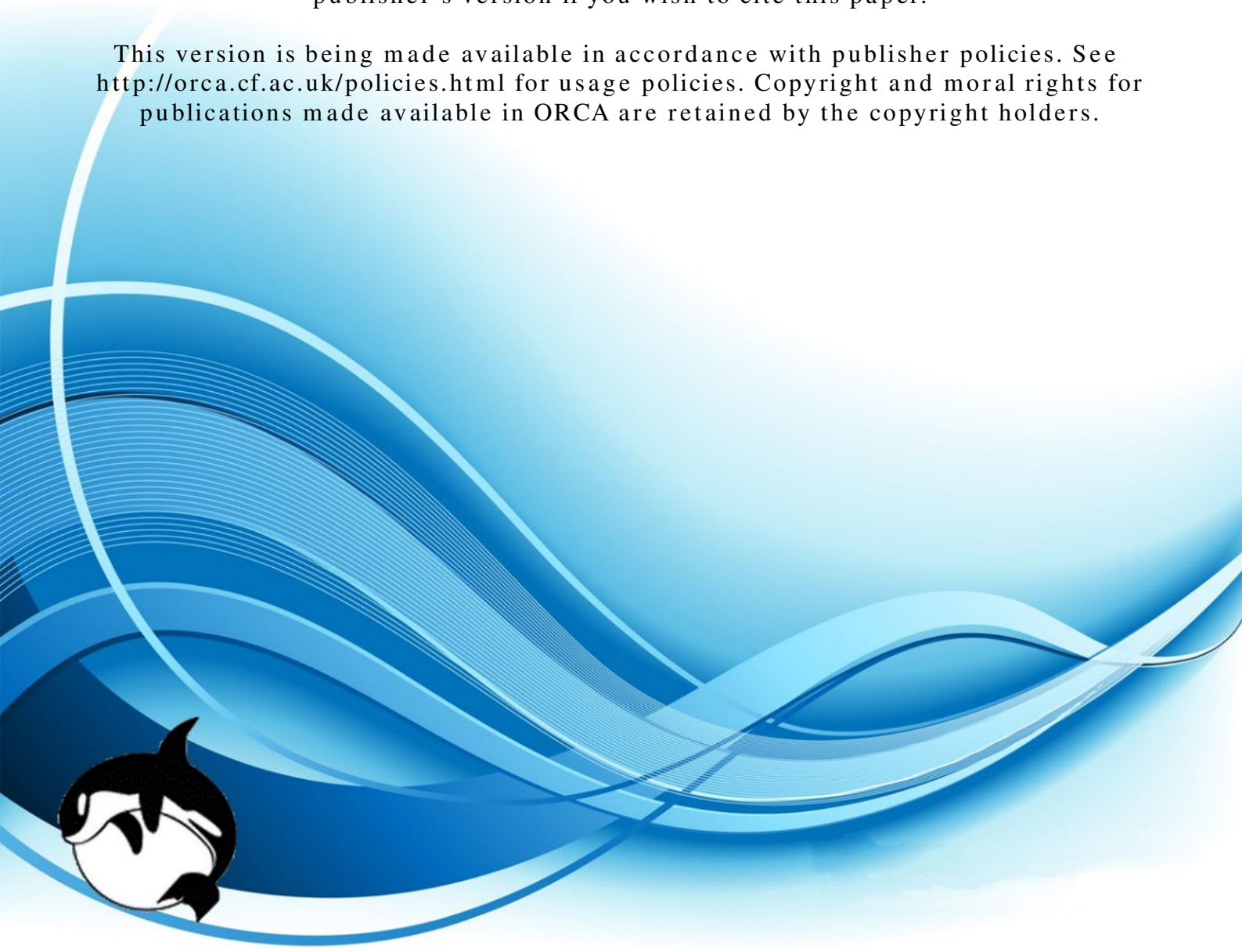

Size of cortical generators of epileptic interictal events and visibility on scalp EEG

Nicolás von Ellenrieder[ab*], Leandro Beltrachini[c], Piero Perucca[a1], and Jean Gotman[a]

[a] Montreal Neurological Institute and Hospital
3801 University Street, Montreal, Quebec, H3A 2B4, Canada

[b] LEICI, Facultad de Ingeniería, Universidad Nacional de La Plata
Calle 1 y 47, La Plata, Buenos Aires, B1900TAG, Argentina.

[c] CISTIB, The University of Sheffield
Sir Frederick Mappin Bldg, Mappin Street, S1 3JD Sheffield, UK

* Corresponding author:
Montreal Neurological Institute
3801 University Street, Room 009d
Montreal, QC H3A 2B4, Canada
nellen@ieee.org
+1 514 398 6644, ext 00445

[1] Persent address:
Departments of Medicine and Neurology
Royal Melbourne Hospital, University of Melbourne
300 Grattan Street, Parkville, Victoria 3050, Australia

Size of cortical generators of epileptic interictal events and visibility on scalp EEG

Abstract

Growing evidence indicates that fast oscillations (>80 Hz) can be recorded interictally in the scalp EEG of patients with epilepsy, and that they may point to the seizure-onset zone. However, mechanisms underpinning the emergence of scalp fast oscillations, and whether they differ from those of interictal epileptic discharges (IEDs), are yet to be understood. The visibility of cortical electric activity on scalp EEG recordings is dependent on two factors: the characteristics of the cortical generator and the background level. We studied this issue using scalp EEG recordings and detailed simulations, with a finite element model including 8 million elements and 8 different tissues. We observed an almost linear relationship between the amplitude of scalp electric potential and the extent of the generator on the cortex. However, this relationship is subject to substantial variability, with variations in factors greater than 3 occurring simply by changing the location on the cortex of generators of fixed extent. In addition, we showed that the background power in scalp EEG recordings decreases at higher frequency bands, being inversely proportional to a power of 2.5 of the frequency. In the specific case of fast oscillations, they can be detected within the lower noise level of the ripple band (80-200 Hz) even though their median amplitude on scalp EEG recordings is more than 10 times smaller than IEDs and consistent with cortical generators of approximately 1 cm^2. In conclusion, the physics governing the propagation of electrical activity from the brain to the scalp are consistent with the hypothesis that scalp fast oscillations and intracranial high-frequency oscillations (HFOs, 80-500 Hz) are expressions of common generators. Given the potential role of HFOs as biomarkers in epilepsy, the possibility to obtain some of the associated information from scalp EEG is of high clinical significance.

Keywords: Fast oscillation; high frequency oscillation; scalp EEG; interictal; focal epilepsy.

Highlights

- Relationship between extent of generators and scalp signal has a large variability.
- Physiological activity decreases with frequency in scalp EEG recordings.
- High frequency generators of small extent can produce visible scalp signals.
- Scalp and intracranial fast oscillations could arise from the same generators.

1. Introduction

Fast oscillations (FO) in scalp EEG recordings have been described in epileptic patients, in pediatric interictal (Wu et al., 2008; Yamazaki et al., 2009) and ictal (Kobayashi et al., 2004; Inoue et al., 2008; Kobayashi et al., 2010) recordings, and more recently in adult interictal recordings (Andrade-Valença et al., 2011; von Ellenrieder et al., 2012; Melani et al., 2013; Zelmann et al., 2013). These interictal scalp FO studies in adults define the FOs as events that stand out of the background, with an approximately sinusoidal shape, and a duration of at least four cycles. The adult studies correspond to three cohorts of focal epilepsy patients, two from the Montreal Neurological Institute and one from the University Medical Center Freiburg, with different filters and sampling rates. In two of the studies the events were marked by different expert neurologists, and in the other two by different semiautomatic detectors. The epileptic origin of these events is evidenced by the fact that in all the studies the FOs occurred in channels also showing Interictal Epileptic Discharges (IED). In fact, scalp FOs were reported to occur in a large proportion at the same time as IEDs, but were less sensitive and more specific than IEDs in identifying the seizure onset zone (Andrade-Valença et al., 2011; Melani et al., 2013).

Mechanisms underlying the emergence of scalp FOs are largely unknown. Specifically, it is unclear whether events seen on scalp correspond to cortical generators producing intracranial high frequency oscillations (HFOs), which have been reported as biomarkers of the seizure onset zone in focal epilepsy (Jacobs et al., 2012; Zijlmans et al., 2012). HFOs are usually seen only in two or three contacts simultaneously in stereo EEG recordings with 5 mm contact separation, and in one or two contacts in subdural recordings with 10 mm contact separation (Wang et al., 2013; Zelmann et al., 2013). This indicates that the generators have a small spatial extent, in the order of 1 or 2 cm^2. For IEDs, an extent of 10 cm^2 has been reported to be necessary for cortical generators to produce visible activity on the scalp (Tao et al., 2007). Then, it would seem unlikely that the small generators associated with intracranial HFOs could produce detectable activity on the scalp. However, the background level decreases at higher frequencies (Freeman and van Dijk, 1987; Freeman et al., 2000; Huigen et al., 2002; Horikawa et al., 2003) improving the visibility of small amplitude events and perhaps facilitating the detection of scalp potentials related to such small generators.

Evidence of a relationship between intracranial and scalp fast activity was recently reported in simultaneous subdural and scalp EEG recordings (Zelmann et al., 2013). In this study, we explore in detail the relationship between the extent of cortical generators and the related electric potential amplitude on the scalp through simulations, and we analyze scalp EEG recordings to determine the

behavior of the noise at different frequencies. Combining the findings we show that recorded scalp FOs could indeed be produced by small cortical generators. Then, the possibility of scalp FOs and intracranial HFOs being related to the same cortical generators cannot be ruled out, and should be further investigated.

2. Methods

We studied the relationship between the extent of the cortical generators and the resulting scalp electric potential distribution through simulations. We solved the Maxwell equations in an extremely detailed head model using the Finite Element Method (FEM). We adopted the usual quasistatic approximation of Maxwell equations (Geselowitz, 1967). This approximation is valid in the head tissues for frequencies up to several kHz (Hämäläinen et al., 1993), meaning that the equations governing the physics of the problem are the same for the whole frequency range in which we are interested.

A detailed head model was built based on the Colin27 high resolution MRI segmentation of the Montreal Neurological Institute (Aubert-Broche et al., 2006). A mesh with more than 8 million tetrahedral elements was created using the iso2mesh software (Fang and Boas, 2009). This resulted in tetrahedra of less than 1 mm side, with local refining in the neighborhood of the cortex. Isotropic conductivity was assumed for 8 tissues included in the model: skin and muscle (0.435 S/m), fat (0.078 S/m), bone (0.0064 S/m), marrow (0.0286 S/m), major blood vessels (0.49 S/m), cerebrospinal fluid (CSF; 1.79 S/m), gray matter (0.333 S/m), and white matter (0.142 S/m). The electric conductivity values were selected from the relevant literature (Bauman et al., 1997; Ramon et al., 2006; Gabriel et al., 2009; Dannhauer et al., 2011; Choi et al., 2012). A slice of the head model showing the mesh and electric conductivity is shown in Fig. 1a. We adopted a geometrically detailed model including many different tissues and isotropic conductivity instead of a coarser model with anisotropic conductivity and the same computational load because for scalp recordings an accurate model of the CSF is more important than the white matter anisotropy (Wolters et al., 2006), and for the skull, modeling hard bone and marrow distinction is more important than modeling the skull anisotropy (Dannhauer et al., 2011).

To model the generators we built a cortical surface as the mid-surface between the CSF - gray matter interface and the gray matter – white matter interface using the Freesurfer software (Dale et al., 1999). We simulated generators only on the cortical surface of the left hemisphere, which was tessellated in more than 330,000 triangular elements. One thousand vertices were randomly selected from the cortical surface as the center location of distributed cortical generators of different spatial extent. The

probability of selecting each vertex was proportional to the area of the surrounding triangles, to avoid a bias toward more densely meshed regions. Twenty different spatial extents between 1/8 cm^2 and 32cm^2 were modeled. Each of these distributed generators was modeled as a set of dipoles on the vertices of the cortical surface, with orientation normal to the surface, and a smooth intensity profile weighted by the area of the surrounding triangles (von Ellenrieder et al., 2009). Since the support of the generators was defined using the geodesic distance to the center of the generator, its actual area depends on the curvature of the involved portion of the cortical surface; we computed the exact area on the cortical surface and refer to it as the *cortical extent* of the generators. In experimental studies the extent of a generator is often computed based on the number of channels showing activity on a subdural grid (Tao et al., 2005; Tao et al., 2007; Hashiguchi et al., 2007). For comparison purposes we computed the *subdural extent* of the generators as the area of the projection of the generator onto the inside of the skull. To compute this subdural extent we projected the cortical generator on the surface delimiting the inside of the skull, in the direction given by the segment joining the center of the generator and the nearest point on the skull. The subdural extent is then always lower than the cortical extent, especially for generators on sulcal walls. An example of generators and their projection on the skull inner surface can be seen in Fig. 1b.

We computed the electric potential at 329 points on the scalp corresponding to the locations of the 10-5 electrode placement system (Oostenveld and Praamstra, 2001; Jurcak et al., 2007). The 10-10 and 10-20 electrodes are subsets of this system. The computation was done with a Galerking formulation of the FEM, assuming linear variation of the electric potential on each element (Hutton, 2004; Wolters, 2006).

In some cases we added simulated noise to the simulation results, to show examples of the resulting visual effect on the scalp electric potential distribution. The added noise is a simulation of scalp EEG background obtained as the combined effect of 6,000 dipolar sources at random locations on the cortical surface and with normally distributed intensities (de Munck et al., 1992). We define the Signal to Noise Ratio (SNR) as the ratio between the maximum of the absolute value of the electric potential produced by the generator and the standard deviation of the simulated noise on the scalp. The probability of detecting a signal of interest immersed in the noise will depend on the SNR value. The extent of the scalp electric potential distribution for noisy measurements can be defined as the number of channels in which the electric potential related to the generators is sufficiently larger than the noise level. In the case of noiseless simulations, this definition of the scalp extent cannot be used. In this

situation we arbitrarily define the scalp extent of the electric potential distribution as the percentage of channels in which the absolute amplitude of the electric potential is greater than half the maximum.

Another issue of interest was the noise level of scalp EEG measurements at different frequencies. We studied this from scalp EEG recordings of a previous study (Andrade-Valença et al., 2011). In these recordings the events of interest consisted of interictal epileptic activity (IEDs and FOs), and we refer to everything else as noise. Unlike above, where noise was a Gaussian signal, this definition of noise includes all the background brain activity, artifacts, and noise generated by the measuring equipment. The data correspond to 30-minute scalp EEG recordings during non-REM sleep of 15 patients with focal epilepsy. The patients underwent EEG-telemetry investigation at the Montreal Neurological Institute (MNI). The study was approved by the MNI and Hospital Research Ethics Committee and all patients signed an informed consent. The clinical purpose of EEG-telemetry included determination of seizure classification and epilepsy syndrome, and pre-surgical evaluation. More information regarding the patients can be found in the original study (Andrade-Valença et al., 2011).

Recordings were performed using the Harmonie monitoring system (Stellate, Montreal, Canada), with scalp electrodes placed according to the International 10–20 system, with additional zygomatic electrodes and electrodes at F9/F10, T9/T10, and P9/P10, and reference CPz. The EEG signals were acquired at a 600 Hz sampling rate, with a low pass antialiasing filter with 200 Hz cutoff frequency. As in the original study, the measurements were processed in a 31-channel bipolar montage.

Two of the 15 patients had long bursts of almost continuous high frequency interictal epileptic activity. We excluded them from the analysis since the aim was to study the noise behavior, and in these patients the contribution of the events of interest represented a noticeable fraction of the total power. In the remaining patients the combined duration and energy of the interictal events was negligible compared to the noise. Additionally, some channels were excluded due to malfunction or continuous artifacts. This resulted in a total of 375 channels from 13 patients.

The power line interference was removed from the recordings using adaptive filtering phased locked to the power line frequency (60 Hz) and its harmonics. Then, we computed the noise power spectral density (PSD) to analyze the variations of noise level with frequency. We estimated the PSD of each channel with a weighted periodogram using Welsh method (Hamming window, 50% overlap), with 0.5 Hz frequency resolution, averaging the whole 30 minutes recordings.

Finally, we studied the signals corresponding to scalp interictal events in order to investigate the possible associated cortical generators. This was done with the same recordings as the noise analysis.

Epileptic interictal events consisting of IEDs (1-40 Hz), fast gamma (40-80 Hz) and ripple (80 – 200 Hz) oscillations had been previously marked by a human expert in the above mentioned scalp EEG recordings (Andrade-Valença et al., 2011). We did an analysis of the SNR of these events in a total of 9 frequency bands of roughly the same relative bandwidth; 10 – 15 Hz, 15 – 20 Hz, 20 – 30 Hz, and 30 – 40 Hz for IEDs, 40 – 60 Hz and 60 – 80 Hz for fast gamma oscillations, and 80 – 120 Hz, 120 – 160 Hz, and 160 – 200 Hz for ripple oscillations. More than 22,000 events had been marked in the 375 channels. We computed the SNR of every event in each subband, and assigned the event to the subband with the highest SNR. The precise timing and duration of the event were automatically selected to maximize the average power of the event. A constraint was imposed on the minimum duration of the events of 4 cycles of the center frequency of the band. The duration of a background window before and after the event was also selected automatically for each event, from a range between 1 and 8 times the period of the central frequency of the band, as the one which maximized the SNR.

To analyze the possible generator extent of the interictal events, the root mean square (RMS) amplitude of the events was computed as the square root of the average power. The relationship between generator extent and amplitude found through the simulations could then be applied to obtain a hypothetical extent for the generators of the real interictal events.

3. Results

3.1. Generator extent and scalp potential

The relationship between generator extent and scalp electric potential amplitude is shown in Fig. 2. A scatter plot of the maximum absolute value of the electric potential vs. cortical generator extent for each of the 20000 simulated generators is show in Fig. 2a, and vs. the subdural generator extent in Fig 2b. The median of the scalp electric potential amplitude for the tested cortical generators is approximately proportional to the cortical generator extent to a power of 0.76, and to the subdural extent to a power of 0.9, i.e. there is an almost linear relationship between the amplitude of the electric potential on the scalp and the extent of the projection of the generator on the inside of the skull. Fig. 2c shows the relative variability of the amplitude with respect to this general behavior, showing the ratio between the 95^{th} and 5^{th} percentiles, which is almost constant for the cortical generator extent, but decreases a little for generators with larger subdural extent.

The maximum amplitude of scalp EEG recordings also depends on the distance between neighboring electrodes. A sparse electrode distribution will in many cases miss the maximum value of the electric potential distribution on the scalp. The results shown in Fig. 2 correspond to the 10-5 electrode system, with 329 electrodes. For the same computations considering fewer electrodes, we found a mean loss in the maximum recorded amplitude of around 10% for a 10-10 system (71 electrodes), and of 25% for a 10-20 system (19 electrodes). These results were independent of the generator extent.

While the previous results show the relationship between the amplitude of the scalp potential and the generator extent, in Fig. 3a we focus on the relationship between the generator extent and the extent of the scalp signal for noiseless simulations. Contrary to what may be expected, we see a decrease in the median of the scalp extent for increasing cortical or subdural extent. This decrease in the scalp extent of noiseless simulations is mostly due to generators centered on sulcal walls. As the extent of these generators grows, they can extend to the opposite wall of the sulci and partially cancel the current density. For generators on the gyri the electric potential distribution on the scalp remains more or less similar in the absence of noise when their cortical extent changes. These generators centered on the gyri roughly correspond to the 10^{th} percentile of the 1000 generators at different locations showing almost no change in the noiseless scalp extent in Fig. 3a. One example of such a generator is shown in Fig. 3b-f. The scalp electric potential distribution of a generator of 10 cm^2 subdural extent (20 cm^2 cortical extent) is shown in Fig. 3b, and the scalp potential of a generator of 1.1 cm^2 subdural extent (1.4 cm^2 cortical extent), centered at the same point on the cortical surface is shown in Fig. 3d. While the shape of the distribution is very similar for both generators, there is a difference of almost an order of magnitude in the amplitude (note the different color scales). The effect of additive noise is shown in the remaining panels. Fig. 3c shows the scalp potential of the large generator with added noise (SNR=3, where the signal is the maximum amplitude of the scalp potential). If the same *absolute* amount of noise is added to the scalp potential of the small generator, the distribution and detection probability are severely affected (Fig. 3e). But if the noise level is lower, so as to maintain the same SNR (Fig. 3f), the detection probability and scalp extent (i.e. the number of channels in which the amplitude is sufficiently larger than the noise level) are almost equal for both generators. This example highlights the direct relationship between the SNR and the detection probability and spatial extent of the scalp events.

3.2. Noise characterization in scalp EEG measurements

The PSD of the scalp EEG measurements is shown in Fig. 4. The behavior is similar in the 375 channels, with variations in the absolute level. The PSD of all the channels is shown in grey, and the median as a

solid black line. At low frequencies, the PSD can be approximated by a power law; the median of the EEG power is proportional to the frequency to a power of -2.5, shown as a black dotted line in Fig. 4. At higher frequencies the power spectral density can be approximated by the same power law plus a constant term of value .002 $(\mu V)^2/Hz$, shown in the figure as a light gray dashed line. This constant term is due mostly to the electronic noise of the amplifiers. It is equivalent to 45 $nV/Hz^{1/2}$, and could be lowered significantly with recent technological improvements (Scheer et al., 2011). The deviations of the median PSD with respect to this approximation are due to the brain rhythms in the range from 3 to 20 Hz, and to the various filters of the acquisition system (high pass filter near 1 Hz, antialiasing filter at 200 Hz, and notches in the power line frequency and harmonics).

3.3. Characterization of interictal events in scalp EEG measurements

The SNR of interictal events in different frequency bands is shown in Fig. 5. The 9 frequency bands cover IEDs (10 – 40 Hz), fast gamma oscillations (40 – 80 Hz), and ripple oscillations (80 – 160 Hz). The number of events in each frequency band is printed above the boxes. The detectability threshold is around two, indicating that the weakest detected events had usually twice the amplitude of the background, regardless of the frequency band. The median of the signal to noise ratio in the different frequency bands has a maximum of 5 (RMS amplitude of the signal 5 times larger than the background level) for the IEDs in the gamma band (20 – 40 Hz), and a minimum of about 3 for the highest frequency subband of the ripple band (160 – 200 Hz). The relatively stable median SNR across frequencies may seem unexpected, but it simply indicates that in all the frequency bands the distribution is skewed, with more weak events with SNR slightly larger than the detection threshold, so the median will not be much larger than this threshold. Note that the highest SNR values do show an important decrease for higher frequency bands. This means that strong IEDs stand out of the background more clearly than FOs, but there is relatively low proportion of strong IEDs in each frequency band and they affect the median minimally.

We also computed the hypothetical relative extent of the generators associated with the interictal events. This was done by computing the median amplitude value of the 350 events with highest RMS amplitude in each frequency band; we selected 350 events since this was roughly the smallest number of events in a band and it allowed having the same number of events in all bands. This median amplitude was raised to a power of 0.76 to obtain the cortical area and 0.9 to obtain the subdural area, as per our earlier results. This was normalized by the value corresponding to the subband 120 – 160 Hz. The result in Fig. 6 shows that the hypothetical generator extent is almost inversely proportional to the

frequency. Hence, the hypothetical extent of strong IED generators is more than 10 times larger than for ripple oscillations.

4. Discussion

Our findings indicate that there is a large variability in the relationship between the extent of cortical generators and the amplitude of the electric potential distribution they produce on the scalp, and that background activity level in scalp EEG recordings decreases with frequency. As a consequence, some small generators of high frequency activity can produce scalp signals that are as easy to detect as typical IEDs.

A priori, the amplitude of the electric potential on the scalp is expected to be related to the generator extent because a larger cortical volume (or cortical surface area in our generator model) involves larger neuronal populations. This is in agreement with the solid angle formulation given by Gloor (1985), and was confirmed by the simulation results. The average relationship between the scalp electric potential amplitude and the subdural extent is almost linear, more so than with the actual cortical extent of the generators, as seen in Fig. 2. This can be explained by the partial cancellation of the electric field and current densities produced by generators on opposite sulci walls. The total dipolar moment of the generator will then be approximately equal to the generator strength times the subdural area, which is closer to an "effective" area than the cortical extent. While the observed general or average behavior is completely expected, there are large variations in the amplitude of the electric potential distribution on the scalp for any given generator extent.

The relative variability of the amplitude as a function of the generator subdural extent is a little higher for smaller generators as seen in Fig. 2c. For small generators there will be a large difference in the involved cortical area and total generator strength between generators on the sulci walls, with subdural extent much smaller than the actual cortical extent, and on the gyri, with similar subdural and cortical extents. A very large variability has been reported for small artificial generators (Cooper et al., 1965). Bigger generators usually include both gyri and sulci so the effect is less noticeable, but even for large generators the proportional variability remains higher than 300%. As can be seen in Fig. 2, this means e.g. that 5% of the generators with a subdural extent of 4 cm^2 will produce a higher scalp potential than half of the generators of 10 cm^2 subdural extent, or that 5% of the generators with subdural extent of 2 cm^2 will produce a higher scalp potential than 5% of the 10 cm^2 generators. Probable causes of this variability include local variations in the thickness of the skull, distance between the cortical surface and

the skull, and the local curvature and shape of the cortical surface, which influences the current density direction. The use of an extremely detailed head model with a large number of elements to accurately model geometric details, and including more tissues than in standard simulations (such as fat, bone marrow, and blood vessels), probably contributed to the resulting high variability.

Note that the variability analyzed in the previous paragraph is due only to different positions of the simulated generators on the cortex. The actual variability of the scalp potential produced by generators of a given extent is quite probably larger. Note for instance that all the simulated generators have circular support on the cortical surface, i.e. they are circular on the inflated cortex. If for a given generator extent the support shape is varied it will certainly add some variability to the scalp potential.

Another very important aspect that will increase the variability of the electric potential amplitude is the generator strength or intensity. In the simulations we assumed constant strength for all the generators, but this is undoubtedly a simplification. The generator strength in EEG is related to the synchronous activation of spatially organized neuronal populations. The strength could depend on many factors. The generator location could affect the generator strength since different regions of the cortex may present different neuronal density or different degrees of spatial organization of the neuronal populations. The generator strength could also vary with the spatial extent of the generator; the discharges of small populations could be more easily synchronized, increasing the strength per unit area, or a smaller generator could correlate with a lower proportion of neuronal involvement, decreasing the generator strength. Different types of events could also recruit a different proportion of the total neuronal population of a given region, and/or the frequency of the activity could facilitate or discourage temporal synchrony. The degree to which these factors affect the generator strength should be studied in detail, but it is certain that they will introduce some variability. Since the scalp potential amplitude is directly proportional to the generator strength (Geselowitz, 1967) all its variability will directly translate into variability of the scalp electric potential amplitude.

It is well known that the skull acts as a spatial low-pass filter, blurring the electric potential distribution on the scalp as compared to the subdural electric potential distribution. This blurring means that the scalp potential of distributed cortical generators of different extent can have very similar spatial distribution, differing only in amplitude as seen in the example of Fig. 3.

While the general direct relationship between scalp amplitude and generators extent is expected, it must be noted that the noise level is as important as the electric potential amplitude produced by a generator in determining if it will be visible on the scalp. In fact, if the proportion between signal

amplitude and noise level or signal to noise ratio (SNR) is the same for two generators of different extent, both will have the same probability of being detected (example in Fig. 3). In other words, the detectability and scalp extent of a cortical generator in the scalp is directly related to the SNR.

The first conclusion we can draw then is that there is a large variability in the extent of generators producing detectable scalp activity. This suggests that results reporting the minimum extent necessary to detect scalp activity (Cooper et al., 1965; Tao et al., 2007; Hashiguchi et al., 2007) should not be interpreted as hard limits. In fact, the original work of Tao et al. (2005) studying the extent of IED generators reported scalp events associated to a few generators of extent between 6 and 10 cm^2 and to most of the generators of extent between 10 to 20 cm^2. This threefold range (6 to 20 cm^2) for the detection limit is consistent with the variability observed in our simulation results.

As discussed above, the other factor affecting the detectability of events in scalp EEG recordings is the noise. The most important contributions to the noise are the electric potential generated by background brain activity, i.e. neuronal activity unrelated to the generator under study, electrochemical activity originating in the interface between the electrode and the skin, and electronic noise generated by the measuring amplifiers (Horikawa et al., 2003). The background brain activity predominates at usual clinical EEG frequencies, and it decreases for increasing frequencies. The electronic noise of the amplifier also has a component inversely proportional to the frequency, but at clinical frequencies it is negligible compared to the electrode-skin electrochemical contact noise (Huigen et al., 2002), which in turn is lower than the background scalp EEG activity (Horikawa et al., 2003). Electromyographic artifacts can interfere with the detection of scalp potential of neuronal origin, but if the artifacts are not frequent they can only affect a small proportion of the events under study. The recordings analyzed correspond to non-REM sleep, minimizing the presence of artifacts.

The noise PSD in our scalp recordings is inversely proportional to the frequency to a power of 2.5, as seen in Fig. 4. This is in concordance with intracranial EEG recordings (Freeman and van Dijk, 1987; Freeman et al., 2000). As the frequency increases and the background activity level decreases, the electronic noise of the amplifiers becomes predominant. In our recordings both factors are equal at approximately 100 Hz, but the level of electronic noise can be reduced further with low noise and low impedance amplifiers built with current technology (Scheer et al., 2011) enabling the measurement of higher frequency activity on the scalp (Waterstraat et al., 2012; Fedele et al., 2012). The electronic noise power spectral density is constant at these frequencies. Hence, the brain activity in the scalp will be masked by the electronic noise at frequencies higher than a few hundred Hertz. In summary, the noise

level decreases rapidly at low frequencies, and it is constant for frequencies higher than approximately 200 Hz. This makes difficult the detection of higher frequency activity on the scalp, e.g. fast ripples (250-500 Hz).

The analysis of the interictal events in Fig. 5 shows that the median of the signal to noise ratio in the different frequency bands has a maximum of 5 in the 20 – 40 Hz band. The SNR decreases in the lowest frequency bands due to the increase of the background activity level generated by the brain rhythms, especially in the 10-15 Hz band as can be seen in Fig. 4. The decrease of SNR in the high frequency bands is due in part to the higher relative contribution of the electronic noise of the amplifiers. In the figure we can see that at approximately 90 Hz half of the noise power is due to the background activity (shown as a dotted line) and the other half to the amplifiers noise. This indicates that if the signal to background brain activity level were similar in different frequency bands, the SNR in the 80 – 120 Hz band would be 70% of the value in the low gamma band (30 – 40 Hz). The difference in the median of the SNR between these bands is indeed close to this value, but the difference in the SNR of the strongest events is higher, suggesting that there is also some decrease in the signal to background brain activity level for higher frequency bands.

The number of events in each frequency band is related to the SNR of the events in that band, with variations among bands much more important than the variations in SNR. Note that in each frequency band, regardless of the maximum SNR values, there are always weak events, barely detectable. This indicates that there is a continuum of possible amplitudes for the events, and in each band only the ones with amplitude large enough as to stand out of the noise are detected. Hence, the number of events in the ripple band is quite probably much larger, but only the strongest ones are detected in the scalp. This would be consistent with scalp FO being related to intracranial HFO generators, since the rate of intracranial HFOs was higher than that of scalp FOs in patients with simultaneous recordings (Zelmann et al., 2013).

Given the high sensitivity of the number of detected events to the SNR, even a minor improvement in SNR could drastically increase the number of detected events. A practical way to accomplish it in our setup would be by using denser electrode covering on the scalp. The halving of the interelectrode distance associated with a change from 10-20 to 10-10 based electrode systems would increase the SNR by 20% according to the simulation results, which would lead to a large increase in the number of detectable events, as suggested by the results shown in Fig. 5. These results agree with the findings reported by Zelmann et al. (2013), in which the scalp activity resulting from simulated 1 cm2 generators

was visible with a 10-20 electrode placement five times less frequently than in a high density EEG system with 256 electrodes.

Even though the median SNR values change by a factor lower than 2 among the frequency bands, both the noise level and the amplitude of the signals are several times lower for the high frequency bands. This lower signal amplitude could be related to smaller generator extents. A rough idea of the possible extent of the generators of the scalp FOs was shown in Fig. 6. It suggests that if a fixed deterministic relationship between amplitude and generator extent is adopted, the average extent of the strongest ripple oscillations will be up to 20 or 30 times smaller than the average generator extent of the strongest IEDs. Note that to arrive to this result we only made use of the RMS amplitude of actual events in scalp EEG recordings and of an assumption of almost linear relationship between scalp electric potential amplitude and generator extent, which was obtained from simulations but is totally reasonable. The fact that these low amplitude events are detectable is simply related to the lower noise level of the higher frequency bands. This is certainly an oversimplification, and large deviations from this average result could be expected. Even so, a 20 times ratio between the generator extent of strong IEDs and strong scalp ripple oscillations is consistent with values found in the literature if we assume that the generators for the scalp and intracranial ripple oscillations are the same. Strong IEDs are probably associated to generators of more than 20 cm^2 subdural extent (Tao et al., 2007), and intracranial generators of strong ripples have probably areas between 1 and 2 cm^2 (Wang, 2013). Evidence of scalp activity associated to small cortical generators was also found by Zelmann et al. (2013) in simultaneous scalp and subdural EEG recordings.

In conclusion, we found no evidence against the hypothesis that scalp FOs are related to cortical generators of small spatial extent. The simulations show that the physics governing the problem do not impose any hard limit on the extent of generators that can produce visible activity on the scalp, and the analyzed interictal events are consistent with the mentioned hypothesis. The amplitude of the interictal events recorded at higher frequency bands is more than 10 times smaller than the amplitude of IEDs, which would be expected if the underlying cortical generators were smaller. The fact that small generators can produce visible scalp potentials can be explained in part by the variability in the relationship between scalp amplitude and generator extent, and in part because the noise is lower in the higher frequency bands; a fraction of the small cortical generators associated to HFOs would produce significantly larger amplitude than the average, and even if this amplitude is still low it might be detected in the scalp because of the low noise level in the ripple band.

More experimental studies are certainly needed to further investigate the possible relationship between the generators of scalp FOs and intracranial HFOs. Given the potential use of intracranial HFOs as biomarkers in epilepsy (Jacobs et al., 2012; Zijlmans et al., 2012), the possibility of obtaining at least part of the same information from non-invasive recordings is of great interest by the very important impact it could have in the clinical evaluation of epilepsy.

Acknowledgement

This work was funded by the Canadian Institute of Health Research (CIHR) grant MOP-10189, Argentina ANPCyT grant PICT 2011-0909, and Universidad Nacional de La Plata grant 11-I-166.

References

Andrade-Valença L, Dubeau F, Mari F, Zelmann R, Gotman J. Interictal scalp fast oscillations as a marker of the seizure onset zone. Neurology 2011; 77:524–31.

Aubert-Broche B, Evans AC, Collins DL. A new improved version of the realistic digital brain phantom. NeuroImage 2006; 32(1):138–45.

Baumann SB, Wozny DR, Kelly SK, Meno FM. The Electrical Conductivity of Human Cerebrospinal Fluid at Body Temperature. IEEE Trans Biomed Eng 1997; 44(3):20-23.

Cooper R, Winter AL, Crow HJ, Walter WG. Comparison of Subcortical, Cortical and Scalp Activity Using Chronically Indwelling Electrodes in Man. Electroencephalogr Clin Neurophysiol 1965; 18:217-228.

Choi HW, Jansen B, Zhang ZD, Kassab, GS. Impact of surrounding tissue on conductance measurement of coronary and peripheral lumen area. J. R. Soc. Interface 2012: published online.

Dale AM, Fischl B, Sereno MI. Cortical Surface-Based Analysis I: Segmentation and Surface Reconstruction. NeuroImage 1999; 9(2):179-194.

Dannhauer M, Lanfer B, Wolters CN, Knösche, TR. Modeling of the Human Skull in EEG Source Analysis. Human Brain Mapping 2011; 32:1383–1399.

de Munck JC, Vijn PCM, Lopes da Silva FH. A random dipole model for spontaneous brain activity. IEEE Trans Biomed Eng 1992; 39:791–804.

Fang Q, Boas D. Tetrahedral mesh generation from volumetric binary and gray-scale images. Proc. of IEEE International Symposium on Biomedical Imaging 2009; 1142-1145.

FedeleT, Scheer HJ, Waterstraat G, Telenczuk B, Burghoff M, Curio G. Towards non-invasive multi-unit spike recordings: Mapping 1 kHz EEG signals over human somatosensory cortex. Clin Neurophysiol 1012; 123:2370–2376.

Freeman W, van Dijk BW. Spatial patterns of visual cortical fast EEG during conditioned reflex in a rhesus monkey. Brain Res 1987; 422:267-276.

Freeman WJ, Rogers LJ, Holmes MD, Silbergeld DL. Spatial spectral analysis of human electrocorticograms including the alpha and gamma bands. Journal of Neuroscience Methods 2000; 95:111–121.

Gabriel C, Peyman A, Grant EH. Electrical conductivity of tissue at frequencies below 1 MHz. Phys Med Biol 2009; 54:4863–4878.

Geselowitz DB. On Bioelectric Potentials in an Inhomogeneous Volume Conductor. Biophys J 1967; 7(1):1–11.

Gloor P. Neuronal Generators and the Problem of Localization in Electroencephalography: Application of Volume Conductor Theory to Electroencephalography. J Clin Neurophysiol 1985; 2(4):327-354.

Hämäläinen M, Hari R, Ilmoniemi R, Knuutila J, Lounasmaa O. Magnetoencephalography--theory, instrumentation, and applications to noninvasive studies of the working human brain. Rev Mod Phys 1993; 65:1-93.

Hashiguchi K, Morioka T, Yoshida F, Miyagi Y, Nagata S, Sakata A, et al. Correlation between scalp recorded electroencephalographic and electrocorticographic activities during ictal period. Seizure 2007; 16:238-247.

Horikawa M, Harada H, Yarita M. Detection Limit in Low-amplitude EEG Measurement. J Clin Neurophysiol 2003; 20(1):45–53.

Huigen E, Peper A, Grimbergen CA. Investigation into the origin of the noise of surface electrodes. Med Biol Eng Comput 2002; 40:332-338.

Hutton DV. Fundamentals of Finite Element Analysis. The McGraw-Hill Companies 2004.

Inoue T, Kobayashi K, Oka M, Yoshinaga H, Ohtsuka Y. Spectral characteristics of EEG gamma rhythms associated with epileptic spasms. Brain Dev 2008; 30:321–8.

Jacobs J, Staba R, Asano E, Otsubo H, Wu JY, Zijlmans M, et al. High-frequency oscillations (HFOs) in clinical epilepsy. Progress in Neurobiology 2012; 98(3):302-315.

Jurcak V, Tsuzuki D, Dan I. 10/20, 10/10, and 10/5 systems revisited: Their validity as relative head-surface-based positioning systems. Neuroimage 2007; 34:1600–1611.

Kobayashi K, Oka M, Akiyama T, Inoue T, Abiru K, Ogino T, et al. Very fast rhythmic activity on scalp EEG associated with epileptic spasms. Epilepsia 2004; 45:488–96.

Kobayashi K, Watanabe Y, Inoue T, Oka M, Yoshinaga H, Ohtsuka Y. Scalp-recorded high-frequency oscillations in childhood sleep-induced electrical status epilepticus. Epilepsia 2010; 50:2190–4.

Melani F, Zelmann R, Dubeau F, Gotman J. Occurrence of scalp-fast oscillations among patients with different spiking rate and their role as epileptogenicity marker. Epilepsy Res 2013; 106(3):345-356.

Oostenveld R, Praamstra P. The five percent electrode system for high-resolution EEG and ERP measurements. Clin Neurophysiol 2001; 112:713–719.

Ramon C, Schimpf PH, Haueisen J. Influence of head models on EEG simulations and inverse source localizations. BioMedical Engineering OnLine 2006; 5:10.

Scheer HJ, Fedele T, Curio G, Burghoff M. Extension of non-invasive EEG into the kHz range for evoked thalamocortical activity by means of very low noise amplifiers. Physiol Meas 2011; 32:N73–N79.

Tao JX, Ray A, Hawes-Ebersole S, Ebersole JS. Intracranial EEG substrates of scalp EEG interictal spikes. Epilepsia 2005; 46(5):669-676.

Tao JX, Baldwin M, Hawes-Ebersole S, Ebersole JS. Cortical substrates of scalp EEG epileptiform discharges. J Clin Neurophysiol 2007; 24:96–100.

von Ellenrieder N, Valdés-Hernández PA, Muravchik CH. On the EEG/MEG forward problem solution for distributed cortical sources. Med Biol Eng Comput 2009; 47(10):1083-1091.

von Ellenrieder N, Andrade-Valença LP, Dubeau F, Gotman J. Automatic detection of fast oscillations (40-200 Hz) in scalp EEG recordings. Clin Neurophysiol 2012; 123(4):670-680.

Wang S, Wang IZ, Bulacio JC, Mosher JC, Gonzalez-Martinez J, Alexopolus AV, et al. Ripple classification helps to localize the sizure-onset zone in neocortical epilepsy. Epilepsia 2013; 54(2):370-376.

Waterstraat G, Telenczuk B, Burghoff M, Fedele T, Scheer HJ, Curio G. Are high-frequency (600 Hz) oscillations in human somatosensory evoked potentials due to phase-resetting phenomena? Clin Neurophysiol 2012; 123:2064–2073.

Wolters CH, Anwander A, Tricoche X, Weinstein D, Koch MA, MacLeod RS. Influence of tissue conductivity anisotropy on EEG/MEG field and return current computation in a realistic head model: A simulation and visualization study using high-resolution finite element modeling. NeuroImage 2006; 30(3):813-826.

Wu JY, Koh S, Sankar R, Mathern GW. Paroxysmal fast activity: an interictal scalp EEG marker of epileptogenesis in children. Epilepsy Res 2008; 82:99–106.

Yamazaki M, Chan D, Tovar-Spinoza Z, Go C, Imai K, Ochi A, et al. Interictal epileptogenic fast oscillations on neonatal and infantile EEGs in hemimegalencephaly. Epilepsy Res 2009; 83:198–206.

Zelmann R, Lina JM, Schulze-Bonhage A, Gotman J, Jacobs J. Scalp EEG is not a blur: it can see High Frequency Oscillations although their generators are small. Brain Topography 2013; in press.

Zijlmans M, Jiruska P, Zelmann R, Leijten FSS, Jefferys JGR, Gotman J. High-frequency oscillations as a new biomarker in epilepsy. Annals of Neurology 2012; 71(2):169-178.

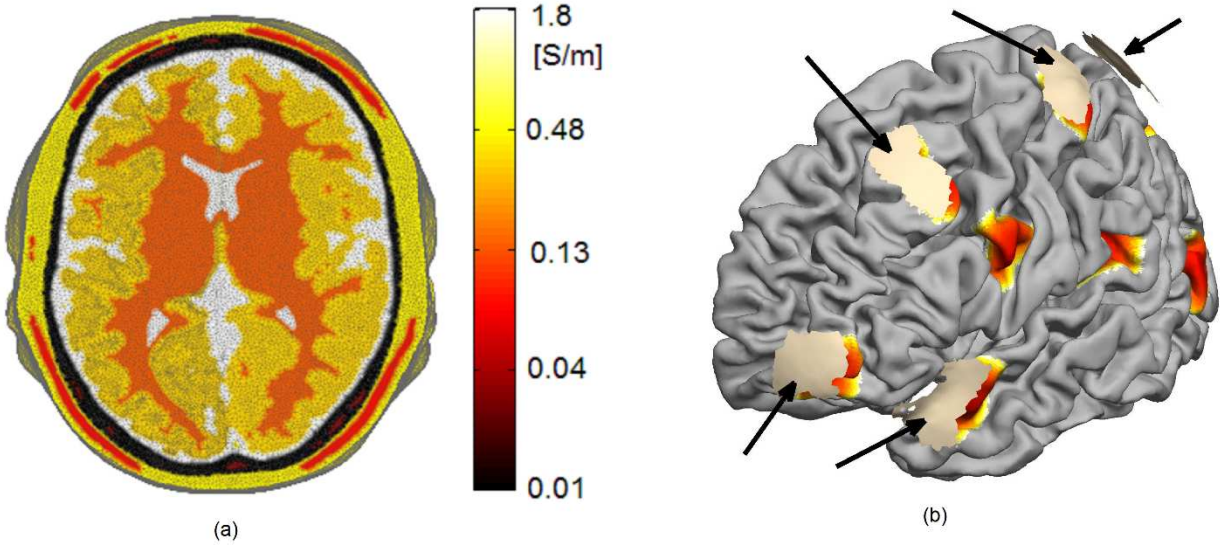

Figure 1: Head model used in the simulations. (a) Electrical conductivity of the model in a slice of the head. The local refining of the mesh can be seen in the left hemisphere gray matter. The color scale saturates at 1 S/m for clarity reasons, although the CSF conductivity is 1.79 S/m. (b) Cortical surface of the left hemisphere tessellated in more than 330,000 triangles. Examples of several generators of 10cm^2 cortical extent are shown in color. The color is proportional to the intensity of the generators and shows their smooth intensity profile. For some of the generators (arrows) the projection on the inside of the skull, which defines their subdural extent, is also shown.

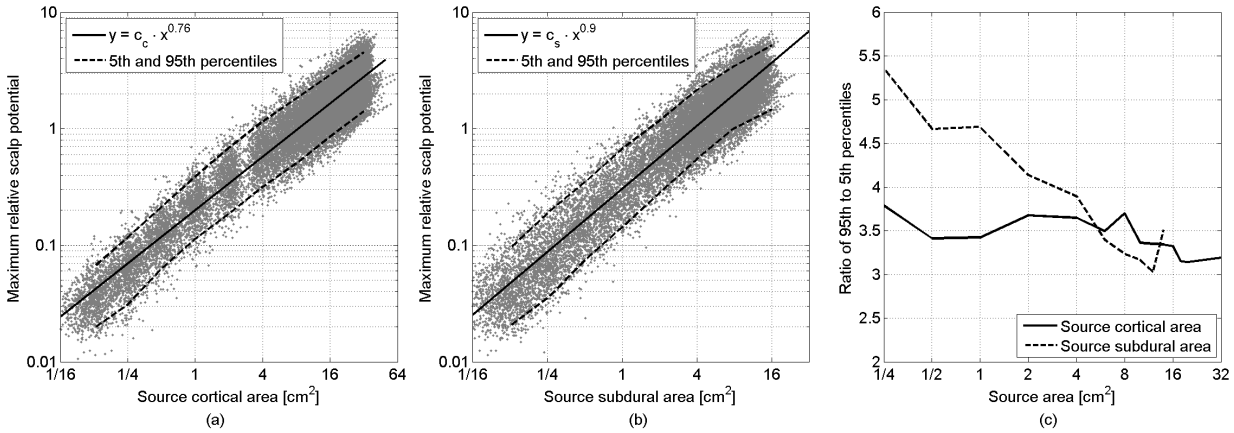

Figure 2: Relationship between extent of the cortical generators and electric potential amplitude on the scalp. (a) Scatter plot of the maximum absolute scalp amplitude versus cortical extent of the generators (20000 different generators as gray dots). The 5th and 95th percentiles are shown as dashed lines, and a power law fit with an exponent of 0.76 as a solid line. The amplitude is shown relative to the median value of generators of 10 cm^2 extent. (b) Idem a, but showing the results as a function of the subdural area of the generators. In this case the exponent of the power law is 0.9. (c) Relative variability of the general behavior shown as the ratio between the 95th and 5th percentiles as a function of the generator extent.

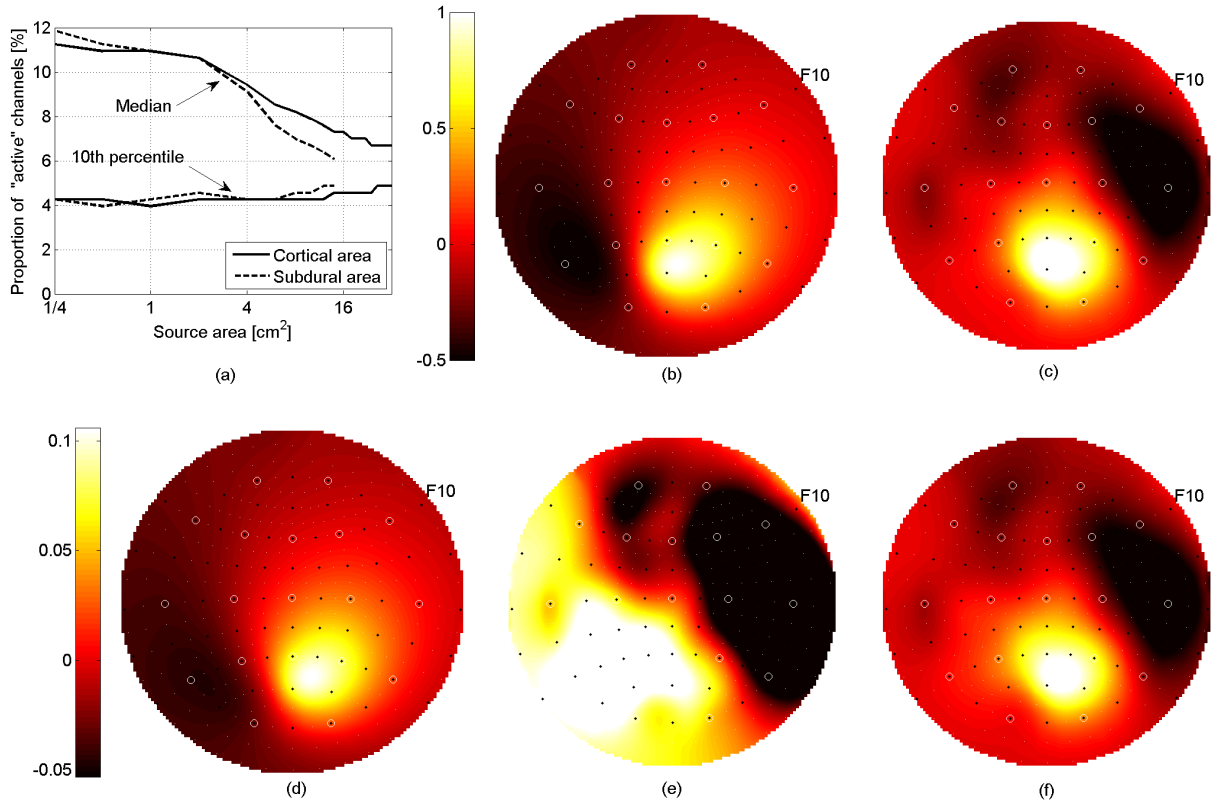

Figure 3: (a) Proportion of channels with absolute amplitude greater than half the maximum. Median and 10th percentile of 1000 cortical generators for each generator area. (b) Normalized electric potential distribution of a generator with subdural extent 10 cm^2. (c) Idem b with additive noise (SNR=3). (d) Electric potential distribution of a generator with subdural extent 1.1 cm^2. (e) Same as d with the same *absolute* noise level as c. (f) Same as d with the same *relative* noise level as c (SNR=3).

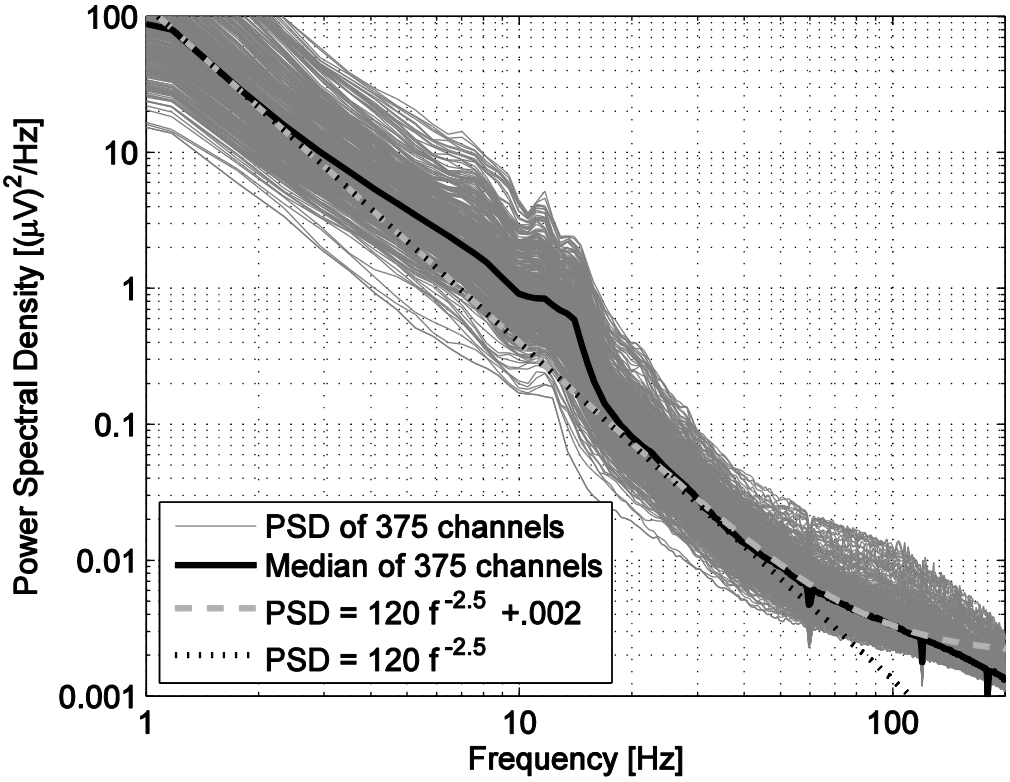

Figure 4: Power spectral density (PSD) of 375 scalp EEG channels during non-REM sleep (grey), median (black full line), and approximations: background brain activity (dotted black line), and background brain activity plus electronic noise (dashed grey line).

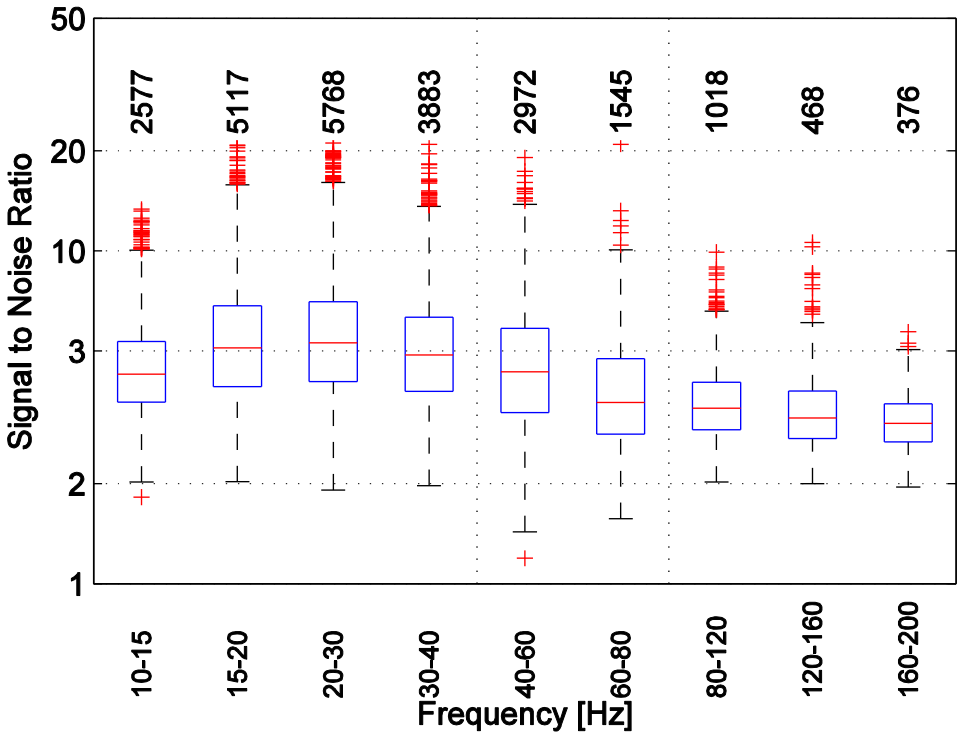

Figure 5: Signal to Noise Ratio distribution of interictal epileptic events in different frequency bands. Median (red line), 25th and 75th percentiles (blue box), outliers (red crosses), and number of events in the frequency band (above).

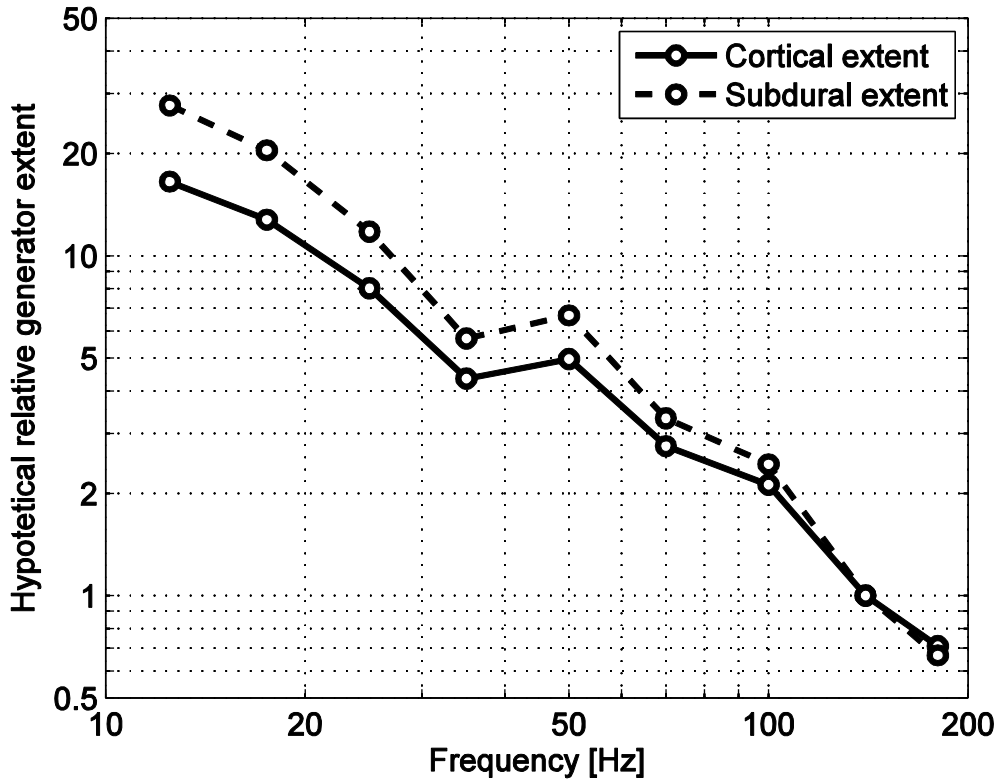

Figure 6: Hypothetical median generator extent of the strongest interictal events as a function of frequency, relative to the median generator extent of the 120 – 160 Hz frequency band.